

Switching properties and domain dynamics of the c -axis polarization in monoclinic $\text{Bi}_4\text{Ti}_3\text{O}_{12}$ single crystals

Yuuki Kitanaka*, Yuji Noguchi***, and Masaru Miyayama*

*Research Center for Advanced Science and Technology, The University of Tokyo,
4-6-1 Komaba, Meguro-ku, Tokyo 153-8505, Japan

Fax: 81-3-5452-5083, e-mail: y-peichun@crm.rcast.u-tokyo.ac.jp

**Solution-Oriented Research for Science and Technology, Japan Science and Technology Agency,
4-1-8 Honcho, Kawaguchi-shi, Saitama 332-0012, Japan

ABSTRACT

We have investigated the domain structures and their dynamics induced by electric field along the c axis in ferroelectric $\text{Bi}_4\text{Ti}_3\text{O}_{12}$ single crystals, taking into account the two spontaneous polarization (P_s) components along the a ($P_{s(a)}$) and c axes ($P_{s(c)}$). Piezoresponse force microscope observations showed that 90° domain walls (composed of the $P_{s(a)}$ component) clamp the motion of $P_{s(c)}$ domain walls, leading to a lower remanent polarization along the c axis. Annealing the crystals under oxidation atmosphere led to not only a complete $P_{s(c)}$ switching without clamped $P_{s(c)}$ domains, but also a marked increase in the coercive field for the $P_{s(c)}$ switching ($E_{c(c)}$). The behavior of $E_{c(c)}$, which cannot be explained by the domain wall pinning attributed to oxygen vacancies, was tentatively interpreted as a result of the interaction between the domain walls composed of $P_{s(c)}$ and electron hole induced by the oxidation treatment.

Key words: bismuth titanate, domain wall, piezoresponse force microscopy, domain pinning

1. INTRODUCTION

Bismuth titanate $\text{Bi}_4\text{Ti}_3\text{O}_{12}$ (BiT), which is a typical member of bismuth layer-structured ferroelectrics, has attracted much attention because BiT shows a large spontaneous polarization (P_s), a high Curie temperature (T_C), and unique electro-optic behaviors.[1-4] Since the crystal structure of BiT has a monoclinic distortion ($B1a1$ space group) in the ferroelectric state,[1, 5] its P_s vector is tilted slightly away from the a axis to the c axis, and the non-zero component of P_s appears along the c axis ($P_{s(c)} \sim 4 \mu\text{C}/\text{cm}^2$) as well as along the a axis ($P_{s(a)} \sim 50 \mu\text{C}/\text{cm}^2$).[1, 6] The P_s vector can be pointed in various directions due to these two switchable components, and the ferroelectric domain structure in BiT is known to contain various types of domain walls (DWs).[1, 7]

Understanding of the static domain structure and its dynamics is an indispensable basis for controlling the properties of the ferroelectric devices. Recently, the domain structure of BiT has been studied using piezoresponse force microscopy (PFM), and the domain structure composed of $P_{s(a)}$ (the major component of P_s) in BiT crystals has been well elucidated.[8, 9] There exists, however, the small but significant component of $P_{s(c)}$ in BiT crystals, and the domain structure is made up of the P_s vector with the two components of $P_{s(a)}$ and $P_{s(c)}$. In this article, we present the domain structures formed by $P_{s(a)}$ and $P_{s(c)}$ in the BiT crystals and their dynamics under electric field along the c axis. $P_{s(c)}$ switching. Polarization measurements and PFM observations provide direct evidence that the presence of

90° DWs composed of $P_{s(a)}$ impede the switching of $P_{s(c)}$, and play a detrimental role in polarization

2. EXPERIMENTAL

BiT single crystals were grown in air by a flux method using BiT powder with excess Bi_2O_3 . [10] The BiT crystals obtained were transparent plate-like sheets with lateral dimensions of approximately $10 \times 10 \text{ mm}^2$ and a thickness of 0.1-0.3 mm along the c axis. The crystals were annealed at 900°C for 10 h in air (air-annealed crystals). Some of the air-annealed crystals were subsequently annealed at 700°C for 10 h at a high oxygen pressure (P_{O_2}) of 35 MPa to reduce the number of oxygen vacancies (high- P_{O_2} -annealed crystals). Figure 1 shows the optical microscope images of (a) an as-grown crystal and (b) an air-annealed crystal. For as-grown crystals, a large number of striped 90° DWs (composed of the $P_{s(a)}$ component) were observed throughout the crystals (Fig. 1(a)). Since annealing at

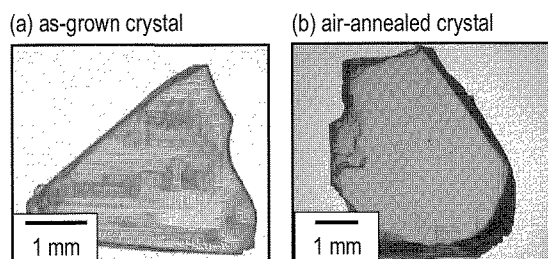


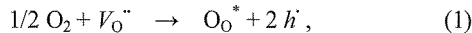
Fig. 1 Optical microscope images of (a) as-grown BiT crystals (90° -DW-rich) and (b) air-annealed crystals (90° -DW-free).

temperatures above T_C drastically reduces the number of the 90° DWs in BiT single crystals,[11] there were only a few 90° DWs in the air-annealed crystals (Fig. 1(b)) and the high- Po_2 -annealed crystals.

For the measurements of electrical properties along the c axis, both major surfaces (the a - b planes) of the crystals were mechanically polished, and then gold electrodes were sputtered onto the polished surfaces. The three kinds of BiT crystals (the as-grown, the air-annealed, and the high- Po_2 -annealed crystals) were subjected to electrical poling before measurements. Unpoled BiT crystals showed an unsaturated polarization hysteresis loop even when a high electric field (E) of 60 kV/cm was applied.[10] For the poling, an E of 60 kV/cm was applied at 150°C to the crystals along the c axis. Optical microscope observations of domain switching were performed to view the domain structures. The detailed domain structure was investigated by PFM on the mechanically polished surfaces of the crystals (the a - b planes).[9]

3. RESULTS AND DISCUSSION

Figure 2 shows the leakage current density (J) as a function of E of the poled crystals along the c axis measured at 25°C . The as-grown crystals exhibited a quite low J of 10^{-10} A/cm². Annealing in air ($\text{Po}_2 = 0.02$ MPa) increased J by about one order of magnitude. The high- Po_2 -annealed crystals exhibited a higher J than the air-annealed crystals. The increase in J caused by the oxygen annealing is attributed to the oxidation reaction as follows:



where $V_{\text{O}}^{\bullet\bullet}$ denotes an oxygen vacancy with two positive charges and O_{O}^* is an oxide ion at the O site. These experimental results lead to the conclusion that the number of $V_{\text{O}}^{\bullet\bullet}$ is decreased by the incorporation of oxygen at the $V_{\text{O}}^{\bullet\bullet}$ during the annealing, and that the leakage current properties along the c axis of the BiT crystals used in this study are governed by electron-hole (h^{\bullet}) conduction (p -type). The p -type conduction has been reported to be responsible also for the electrical conduction along the a axis of BiT.[12, 13]

Figure 3 shows the polarization hysteresis loops of the BiT crystals along the c axis. As a result of the poling, all the hysteresis loops showed the imprint characteristics, with the loops displaced along the positive E axis.[14] The as-grown crystals exhibited an

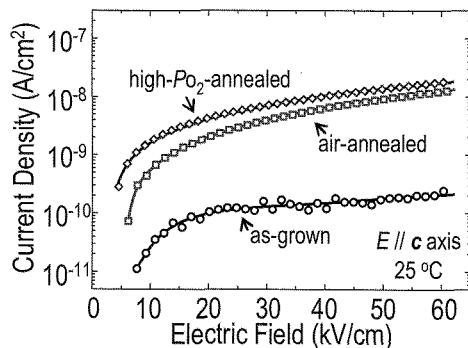


Fig. 2 Leakage current density along the c axis of the BiT crystals annealed under various conditions.

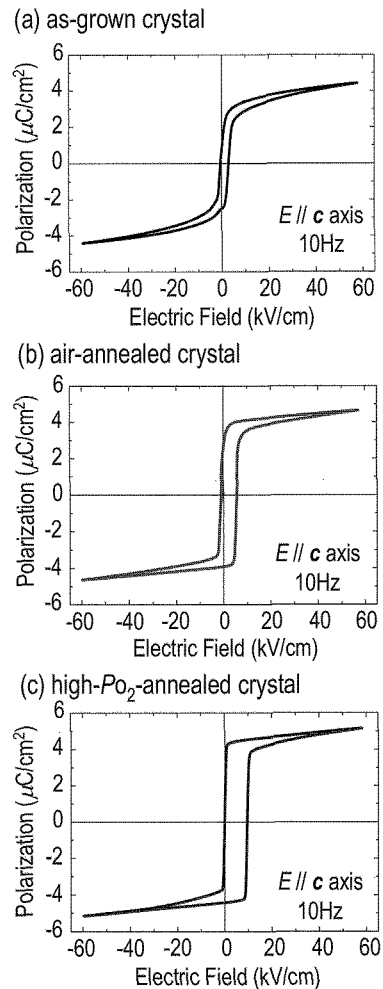


Fig. 3 Polarization properties of poled BiT crystals measured along the c axis at 25°C .

unsaturated hysteresis loop despite having the excellent insulating properties (as shown in Fig. 2), with a remanent polarization along the c axis ($P_{r(c)}$) of $2.2 \mu\text{C}/\text{cm}^2$ and a coercive field ($E_{c(c)}$) of 1.7 kV/cm. In this study, taking into account the imprint characteristics, we estimated the values of $P_{r(c)}$ and $E_{c(c)}$ from the hysteresis loops whose center was set to be the origin. The air-annealed crystals exhibited a well-saturated hysteresis loop with a $P_{r(c)}$ of $4.0 \mu\text{C}/\text{cm}^2$ and an $E_{c(c)}$ of 3.2 kV/cm. The high- Po_2 -annealed crystals had an equivalent $P_{r(c)}$ of $4.4 \mu\text{C}/\text{cm}^2$ compared with the air-annealed crystals. The high- Po_2 annealing led to a significant increase in $E_{c(c)}$, to a value of 4.7 kV/cm. The values of $P_{r(c)}$ measured in the air-annealed and high- Po_2 -annealed crystals are consistent with the value of $P_{s(c)}$, revealing that $P_{s(c)}$ was completely switched in these crystals under an ac E of 60 kV/cm (1 Hz). The smaller $P_{r(c)}$ of the as-grown crystals compared with $P_{s(c)}$ demonstrates that “frozen” domains, i.e. unswitchable domains, are present in the crystals even after applying an E much higher than the $E_{c(c)}$.

Figure 4 indicates switching process of $P_{s(c)}$ domain structure observed on poled high- Po_2 -annealed crystals using a polarizing microscope. We employed the tilted-extinction method[15] to observe the $P_{s(c)}$ switching, where the c axis of the crystal was set at a 30°

angle to the light path of a microscope by tilting the crystal around the a axis. Figure 4(a) shows a photograph of domain structure under an E of 60 kV/cm along the c axis. The symbol beside the photograph indicates the direction of the applied E . The dashed line between bright and dark areas in the photograph was $P_{s(a)}$ -180° DWs ($P_{s(a)}$ directions were opposite between the both sides of the line), which was confirmed by PFM observations.[16] When an E of 60 kV/cm was applied in the opposite direction, bright and dark states were thoroughly reversed as shown in Fig. 4(b). This result indicates that the $P_{s(c)}$ switching was readily achieved in the high- PO_2 -annealed crystals without “frozen” domains. Also in poled air-annealed crystals, unswitchable domains were not observed in similar observations. These results confirmed that the complete switching of $P_{s(c)}$ was achieved in the air-annealed crystals and the high- PO_2 -annealed crystals that exhibited well-saturated polarization hysteresis loops (Figs. 3(b) and 3(c)).

Figure 5 indicates the domain structure of the poled as-grown crystals observed by PFM. Figure 5(a) shows the in-plane PFM image on the a - b plane; the signal intensity of this image is determined by the direction of $P_{s(a)}$. Striped 90° domain structures were observed in this region, as have been reported in Refs. 8 and 9. Optical microscope observations reveal that this 90° domain structure due to $P_{s(a)}$ did not change during the $P_{s(c)}$ switching, which indicates that the $P_{s(c)}$ switching occurs without the motion of the 90° DWs. Figure 5(b) exhibits the out-of-plane PFM image, which visualizes the $P_{s(c)}$ domain structure in the same region as Fig. 5(a). The domain structure of the dotted square in Figs. 5(a) and 5(b) is depicted in Fig. 5(c). The $P_{s(c)}$ domains in this region were not aligned in the same direction even though the poling was conducted at 150°C, which is responsible for the smaller $P_{r(c)}$ of the as-grown crystals (Fig. 3(a)).

Note that the $P_{s(c)}$ domains are separated by the 90° DWs, as can be clearly seen in Fig. 5(c). The boundaries labeled by “1” are the $P_{s(c)}$ DWs as well as the 90° ($P_{s(a)}$) DWs, across which the directions of both the $P_{s(c)}$ and the $P_{s(a)}$ rotate. The schematic three-dimensional domain structure of the DWs labeled by “1” adjacent to the crystal surface is illustrated in Fig. 5(d). In contrast, the boundary labeled by “2” is the $P_{s(c)}$ DW

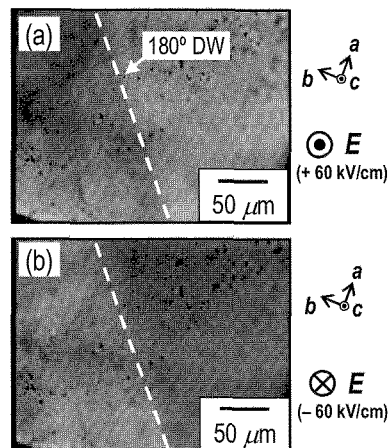


Fig. 4 Photographs of domain structures in the poled high- PO_2 -annealed crystals under E of (a) +60 kV/cm and (b) -60 kV/cm along the c axis.

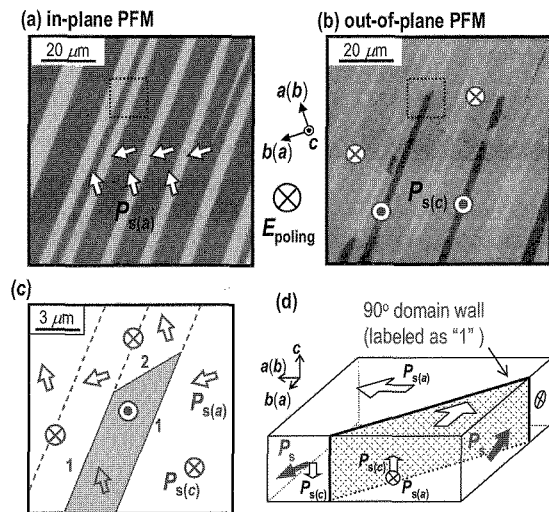


Fig. 5 (a) In-plane PFM image on the a - b surface of poled as-grown BiT crystals, (b) out-of-plane PFM image in the same area, (c) the schematic domain structure of the dotted square. The arrows and the symbols denote the directions of $P_{s(a)}$ and $P_{s(c)}$, respectively. In Fig. 3(c), the dashed line represents 90° ($P_{s(a)}$) DW, the solid line denotes $P_{s(c)}$ domain wall (labeled as “1” and “2”). (d) The schematic three-dimensional domain structure of $P_{s(c)}$ -clamping 90° DW (“1”) adjacent to the crystal surface.

without the change in the direction of $P_{s(a)}$. The presence of the DWs labeled as “1” is direct evidence that the $P_{s(c)}$ switching is impeded by the 90° ($P_{s(a)}$) DWs. For the air-annealed crystals and high- PO_2 -annealed crystals, the electrical measurements were performed on the regions without the 90° DWs (the 90° DWs were few), and then polarization switching was achieved throughout these crystals as clearly shown in Fig. 4. The 90° ($P_{s(a)}$) DWs are found to constitute an obstacle for the $P_{s(c)}$ switching, leading to a lower $P_{r(c)}$ observed for the as-grown crystals.

Here we discuss the origin of the increase in $E_{c(c)}$ by the oxidation treatments in the BiT crystals. The as-grown crystals with a large number of the 90° DWs showed a low $E_{c(c)}$ compared with the 90°-DW-free crystals, i.e. the air-annealed and high- PO_2 -annealed crystals. These results suggest that the 90° DWs do not influence $E_{c(c)}$ by a significant degree but prevent the $P_{s(c)}$ domains from switching. Since the 90° DWs penetrate the crystals along the c axis,[9] the 90° DWs do not affect the forward motion of the $P_{s(c)}$ DWs along the c axis (parallel to external electric field), while the 90° DWs clamp the sidewise motion of the $P_{s(c)}$ DWs along the a and b axes (perpendicular to external E), leading to a lower $P_{r(c)}$ due to an increase in unswitchable domains.[17] It is expected that the presence of the 90° DWs has little influence on the value of $E_{c(c)}$ determined by the dynamic behavior of the switchable domains. These considerations lead to the conclusion that the $E_{c(c)}$ in the BiT system is determined mainly by the mobility of $P_{s(c)}$ DWs along the c axis.

The marked increase in J resulting from the annealing (Fig. 2) provides direct evidence that the oxidation of the crystals decreases the density of $V_O^{\bullet\bullet}$ ($[V_O^{\bullet\bullet}]$) accompanied by an increase in the density of h^{\bullet} ($[h^{\bullet}]$), as expressed in Eq. (1). It has been speculated in perovskite ferroelectrics that $V_O^{\bullet\bullet}$ acts as a pinning center

for preventing DWs from moving to achieve polarization switching by applying an E . [18-20] The mechanism of the DW pinning leading to an increase in E_c would be attributed to a strong V_{O}^{\bullet} -DW interaction, which suppresses the movement of these DWs. In this context, the increase in $[V_{\text{O}}^{\bullet}]$ is likely to enhance “domain pinning”, yielding a higher $E_{c(e)}$ also in the BiT crystals. [21] As shown in Fig. 3, however, the oxidation treatments indeed increased $E_{c(e)}$ for the BiT crystals. The domain pinning by V_{O}^{\bullet} cannot explain this result because the annealed BiT crystals with a lower $[V_{\text{O}}^{\bullet}]$ exhibited a higher $E_{c(e)}$. A possible origin of the higher $E_{c(e)}$ by the oxidation treatments is the interaction between the DWs and h . In fact, the BiT crystals with a higher $[h]$ exhibited a higher $E_{c(e)}$. Luke has reported that the addition of iron to BiT crystals increases $E_{c(e)}$. [22] He has proposed that charge carriers generated by the iron substitution prevent the initial nuclei of E -induced $P_{s(e)}$ domains from growing along the c axis (forward motion of $P_{s(e)}$ DWs). The higher $E_{c(e)}$ induced by the oxidation treatments in the present work agrees well with the Luke’s suggestion that a higher concentration of charge carriers leads to a higher $E_{c(e)}$. During the forward growth of $P_{s(e)}$ domains, head-to-head or tail-to-tail configurations of $P_{s(e)}$ are established in the crystals. These domain configurations possess electrical charge at the boundaries, which interact with charge carrier such as h . The high mobility of h (especially in the a - b plane) [12] compared with V_{O}^{\bullet} at room temperature seems to induce the h -induced pinning of the forward motion of $P_{s(e)}$ DWs in the BiT system. The experimental results in this study are reasonably explained in view of the h -induced pinning of the forward motion of $P_{s(e)}$ DWs and the 90° -DW-induced clamping of the sidewise motion of $P_{s(e)}$ DWs.

4. CONCLUSIONS

The detailed domain structure composed of $P_{s(a)}$ and $P_{s(e)}$ in monoclinic BiT single crystals was observed by PFM, and the polarization properties along the c axis were investigated. It was demonstrated that the 90° DWs composed of $P_{s(a)}$ do not influence E_c for “switchable” domains by a significant degree, but prevent the sidewise motion of $P_{s(e)}$ DWs, resulting in a lower $P_{r(e)}$ due to an increase in “frozen” domains. The domain wall pinning attributed to oxygen vacancies cannot explain the higher $E_{c(e)}$ caused by the oxidation treatments of the crystals, which was tentatively interpreted as a result of

the hole-induced pinning of the forward motion of $P_{s(e)}$ DWs.

REFERENCES

- [1] S. E. Cummins and L. E. Cross, *J. Appl. Phys.*, **39**, 2268-74 (1968).
- [2] E. C. Subbarao, *Phys. Rev.*, **122**, 804-07 (1961).
- [3] B. H. Park, B. S. Kang, S. D. Bu, T. W. Noh, J. Lee and W. Jo, *Nature*, **401**, 682-84 (1999).
- [4] S. Y. Wu, W. J. Takei and M. H. Francombe, *Ferroelectrics*, **10**, 43-46 (1976).
- [5] A. D. Rae, J. G. Thompson, R. L. Withers and A. C. Willis, *Acta Crystallogr.*, **46**, 474-87 (1990).
- [6] H. Irie, M. Miyayama and T. Kudo, *J. Appl. Phys.*, **90**, 4089-94 (2001).
- [7] Y. Ishibashi and M. Iwata, *Jpn. J. Appl. Phys.*, **46**, 272-75 (2007).
- [8] M. Soga, Y. Noguchi, M. Miyayama, H. Okino and T. Yamamoto, *Appl. Phys. Lett.*, **84**, 100-02 (2004).
- [9] S. Katayama, Y. Noguchi and M. Miyayama, *Adv. Mater.*, **19**, 2552-55 (2007).
- [10] Y. Kitanaka, Y. Noguchi and M. Miyayama, *Trans. Mater. Res. Soc. Jpn.*, **32**, 27-30 (2007).
- [11] M. M. Hopkins and A. Miller, *Ferroelectrics*, **1**, 37-42 (1970).
- [12] M. Takahashi, Y. Noguchi and M. Miyayama, *Jpn. J. Appl. Phys.*, **41**, 7053-56 (2002).
- [13] Y. Noguchi, T. Matsumoto and M. Miyayama, *Jpn. J. Appl. Phys.*, **44**, L570-L72 (2005).
- [14] S. H. Kim, D. J. Kim, J. G. Hong, S. K. Streiffer and A. I. Kingon, *Integrated Ferroelectrics*, **22**, 653-62 (1998).
- [15] S. E. Cummins and T. E. Luke, *IEEE Trans. Electron Devices*, **ED-18**, 761-68 (1971).
- [16] Y. Kitanaka, S. Katayama, Y. Noguchi and M. Miyayama, *Jpn. J. Appl. Phys.*, **46**, 7028-30 (2007).
- [17] Y. Kitanaka, Y. Noguchi and M. Miyayama, *Appl. Phys. Lett.* **90**, 202904 (2007).
- [18] J. F. Scott and C. A. Paz de Araujo, *Science*, **246**, 1400-05 (1989).
- [19] J. F. Scott and M. Dawber, *Appl. Phys. Lett.*, **76**, 3801-03 (2000).
- [20] L. He and D. Vanderbilt, *Phys. Rev. B*, **68**, 134103 (2003).
- [21] Y. Noguchi, M. Miyayama, K. Oikawa, T. Kamiyama, M. Osada and M. Kakihana, *Jpn. J. Appl. Phys.*, **41**, 7062-75 (2002).
- [22] T. E. Luke, *J. Appl. Phys.*, **45**, 1605-10 (1974).

(Received December 19, 2007; Accepted January 18, 2008)